J/ψ and ψ' suppression by comovers in Pb+Pb collisions

Sean Gavin[a] and Ramona Vogt[bc*]

[a]Physics Department, Brookhaven National Laboratory, Upton, NY

[b]Physics Department, Lawrence Berkeley National Laboratory, Berkeley, CA

[c]Physics Department, University of California, Davis, CA

Measurements of ψ and ψ' production at the CERN SPS are compared to predictions based on a hadronic model of charmonium suppression. Detailed information is presented to facilitate comparison to other analyses. Sensitivity of these conclusions to the model parameters is discussed.

1. INTRODUCTION

Has the quark–gluon plasma been discovered at the SPS? The NA50 collaboration reported a dramatic decrease in ψ production in Pb+Pb collisions at 158 GeV per nucleon [1]. Specifically, M. Gonin presented at this meeting a striking 'threshold effect' in the ψ–to–continuum ratio as a function of a calculated quantity, the mean path length of the ψ through the nuclear medium, L, see fig. 1. This apparent threshold has sparked considerable excitement as it may signal deconfinement in the heavy Pb+Pb system [2].

In this talk we report on work in ref. [3] comparing Pb results to predictions using a hadronic model of charmonium suppression. We first demonstrate that the behavior in the NA50 plot is not a threshold effect but, rather, reflects the approach to the geometrical limit of L as the symmetric Pb+Pb collisions become increasingly central. When plotted as a function of the *measured* neutral transverse energy E_T as in fig. 2, the data varies smoothly as in S+U measurements in fig. 4b below [6–9]. The difference between S+U and Pb+Pb data lies strictly in the relative magnitude. To assess this magnitude, we compare ψ and ψ' data to expectations based on the hadronic comover model [4,5]. The curve in fig. 1 represents our calculation using parameters fixed earlier in Ref. [5]. Our result is essentially the same as the Pb+Pb prediction in [4].

Our primary intention in this work is to demonstrate that there is no evidence for a strong discontinuity between pA, S+U and Pb+Pb data. Secondly, we show that our model predictions agree with the new Pb+Pb data. The consistency of our predictions can be judged by comparing our old pA and S+U calculations with more recent NA38 and NA51 data. However, we must be cautious about taking model details too seriously. Regarding the first point, we quote Maurice Goldhaber: "... absence of evidence is *not*
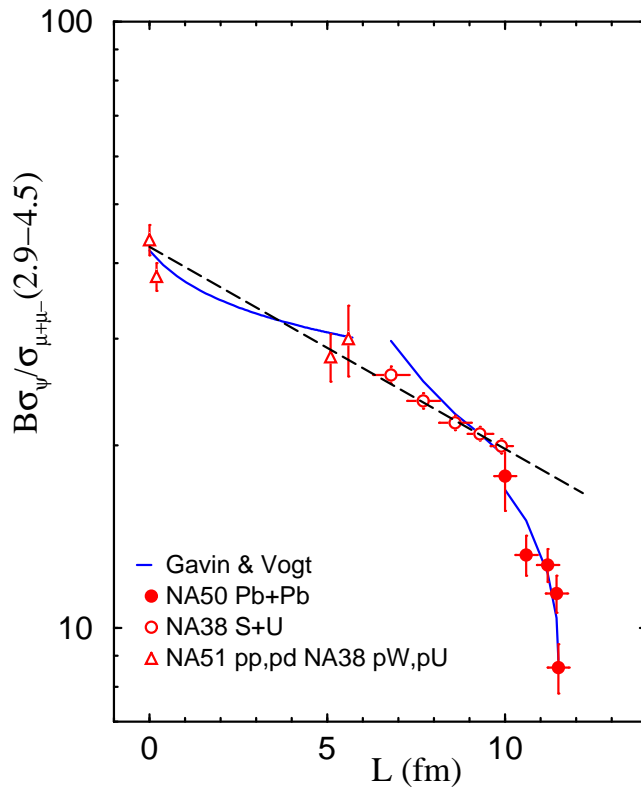
Figure 1. NA50 comparison [1] of Pb+Pb and S+U$\to \psi + X$ as functions of the average path length L, see eq. (3). B is the $\psi \to \mu^+\mu^-$ branching ratio.

evidence of absence." Moreover, we do not attempt to show that our comover interpretation of the data is unambiguous – this is certainly impossible at present. Finally, the significance of our present results must be weighted by the fact that all pA and AB data are preliminary and at different beam energies. Whether the newer data is indeed 'improved' has yet to be established. One should be particularly cautious in taking literally the values of model parameters, such as the comover density.

2. NUCLEONS AND COMOVERS

The hadronic contribution to the suppression arises from scattering of the nascent ψ with produced particles – the comovers – and nucleons [3–5]. To determine the suppression from nucleon absorption, we calculate the probability that a $c\bar{c}$ pair produced at a point (b, z) in a nucleus survives scattering with nucleons to form a ψ. The standard [5,10]
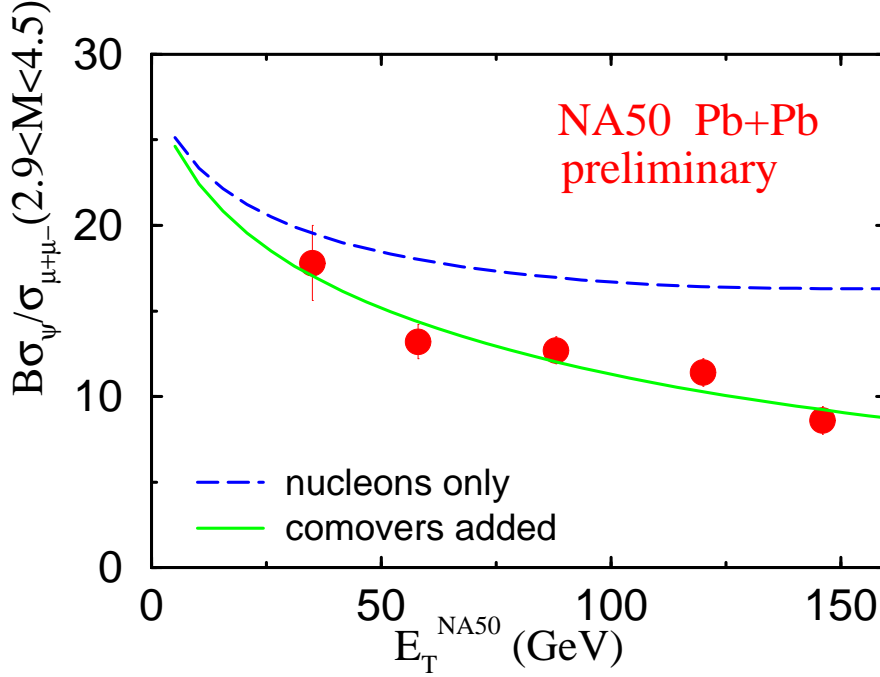
Figure 2. ψ–to–continuum ratio as a function of E_T from [1] compared to the comover prediction [3].

result is

$$S_A = \exp\{-\int_z^{\infty} dz \, \rho_A(b,z)\sigma_{\psi N}\} \tag{1}$$

where ρ_A is the nuclear density, b the impact parameter and $\sigma_{\psi N}$ the absorption cross section for ψ–nucleon interactions. One can estimate $S_A \sim \exp\{-\sigma_{\psi N}\rho_0 L_A\}$, where L_A is the path length traversed by the $c\bar{c}$ pair. On average, L_A cannot exceed the nuclear radius R_A, since the pair can be produced anywhere within the nucleus.

Suppression can also be caused by scattering with mesons that happen to travel along with the $c\bar{c}$ pair (see refs. in [4]). The density of such comovers scales roughly with E_T. The corresponding survival probability is

$$S_{\text{co}} = \exp\{-\int d\tau n \, \sigma_{\text{co}} v_{\text{rel}}\}, \tag{2}$$

where n is the comover density and τ is the time in the ψ rest frame. We write $S_{\text{co}} \sim \exp\{-\beta E_T\}$, where β depends on the scattering frequency, the formation time of the

comovers and the transverse size of the central region, R_T, *cf.* eq. (8).

To understand the saturation of the Pb data with L in fig. 1, we apply the schematic approximation of Ref. [10] for the moment to write

$$\frac{\sigma_\psi^{AB}(E_T)}{\sigma_{\mu^+\mu^-}^{AB}(E_T)} \propto \langle S_A S_B S_{\mathrm{co}} \rangle \sim \mathrm{e}^{-\sigma_{\psi N}\rho_0 L} \mathrm{e}^{-\beta E_T}, \tag{3}$$

where the brackets imply an average over the collision geometry for fixed E_T and $\sigma(E_T) \equiv d\sigma/dE_T$. The path length $L \equiv \langle L_A + L_B \rangle$ and transverse size R_T depend on the collision geometry. The path length grows with E_T, but most stop at the geometric limit $R_A + R_B$ in central collisions. Explicit calculations show that nucleon absorption begins to *saturate* for $b < R_A$, where R_A is the smaller of the two nuclei, see fig. 6 below. On the other hand, particle production and, consequently, E_T continue to grow after L saturates due, *e.g.*, to fluctuations in the number and hardness of NN collisions. Equation (2) falls exponentially in the 'super–central' regime, $b < R_A$, because β is essentially fixed.

Important for understanding the NA50 results is the fact that saturation occurs at larger values of the average impact parameter for Pb+Pb system compared to S+U, see fig. 6 below. This result reflects the striking geometric difference between symmetric and asymmetric nuclear collisions. Specifically, in the S+U system there is large region, $R_S < b < R_S + R_U$, where varying b changes the volume of the interaction region dramatically. In contrast, $R_A = R_B$ in Pb+Pb collisions and $R_{\mathrm{Pb}} \approx 6.6$ fm is large. We show below that typical values of b corresponding to the E_T region covered by NA50 data do not go far into the region $R_{\mathrm{Pb}} < b < 2R_{\mathrm{Pb}}$ where [The importance of b being near zero for saturation to occur was overemphasised in SG's oral presentation of this talk.]

3. J/ψ SUPPRESSION

In fig. 1, we compare the Pb data to calculations of the ψ–to–continuum ratio that incorporate nucleon and comover scattering. The contribution due to nucleon absorption indeed levels off for small values of b, as expected from eq. (3). Comover scattering accounts for the remaining suppression.

These results are *predictions* obtained using the computer code of Ref. [4] with parameters determined in Ref. [5]. However, to confront the present NA50 analysis [1], we must perform the following updates:

- Calculate the continuum dimuon yield in the new mass range $2.9 < M < 4.5$ GeV.

- Adjust the E_T scale to the pseudorapidity acceptance of the NA50 calorimeter, $1.1 < \eta < 2.3$.

The agreement in fig. 1 depends strongly on these adjustments.

We now review the details of our calculations, highlighting the adjustments as we go. For collisions at a fixed b, the ψ–production cross section is

$$\sigma_\psi^{AB}(b) = \sigma_\psi^{NN} \int d^2s\,dz\,dz'\, \rho_A(s, z)\rho_B(b - s, z')\, S \tag{4}$$

where $S \equiv S_A S_B S_{\mathrm{co}}$ is the product of the survival probabilities in the projectile A, target B and comover matter. The continuum cross section is

$$\sigma_{\mu^+\mu^-}^{AB}(b) = \sigma_{\mu^+\mu^-}^{NN} \int d^2s\,dz\,dz'\, \rho_A(s, z)\rho_B(b - s, z'). \tag{5}$$

The magnitude of eqs. (4), (5) and their ratio is fixed by the elementary cross sections σ_ψ^{NN} and $\sigma_{\mu^+\mu^-}^{NN}$. We calculate σ_ψ^{NN} using the phenomenologically–successful color evaporation model [11]. The continuum in the mass range used by NA50, $2.9 < M < 4.5$ GeV, is described by the Drell–Yan process [12]. To confront NA50 and NA38 data in the appropriate kinematic regime, we compute these cross sections at leading order using GRV LO parton distributions with a charm K–factor $K_c = 2.7$ and a color evaporation coefficient $F_\psi = 2.54\%$ from [11] and a Drell–Yan K–factor $K_{DY} = 2.4$. Using these cross sections to construct the normalized ratios in fig. 2 corresponds to the first update.

To obtain E_T dependent cross sections from eqs. (4) and (5), we write

$$\sigma^{AB}(E_T) = \int d^2b\, P(E_T, b)\sigma^{AB}(b). \tag{6}$$

The probability $P(E_T, b)$ that a collision at impact parameter b produces transverse energy E_T is related to the minimum–bias distribution by

$$\sigma_{\min}(E_T) = \int d^2b\, P(E_T, b). \tag{7}$$

We parametrize $P(E_T, b) = C \exp\{-(E_T - \overline{E}_T)^2/2\Delta\}$, where $\overline{E}_T(b) = \epsilon\mathcal{N}(b)$, $\Delta(b) = \omega\epsilon\overline{E}_T(b)$, $C(b) = (2\pi\Delta(b))^{-1}$ and $\mathcal{N}(b)$ is the number of participants (see, $e.g.$, Ref. [4]). We take ϵ and ω to be phenomenological calorimeter–dependent constants.

We compare the minimum bias distributions for total hadronic E_T calculated using eq. (7) for $\epsilon = 1.3$ GeV and $\omega = 2.0$ to NA35 S+S and NA49 Pb+Pb data [13]. The agreement in fig. 3a builds our confidence that eq. (7) applies to the heavy Pb+Pb system. Figure 3b shows the distribution of neutral transverse energy calculated using eqs. (5)
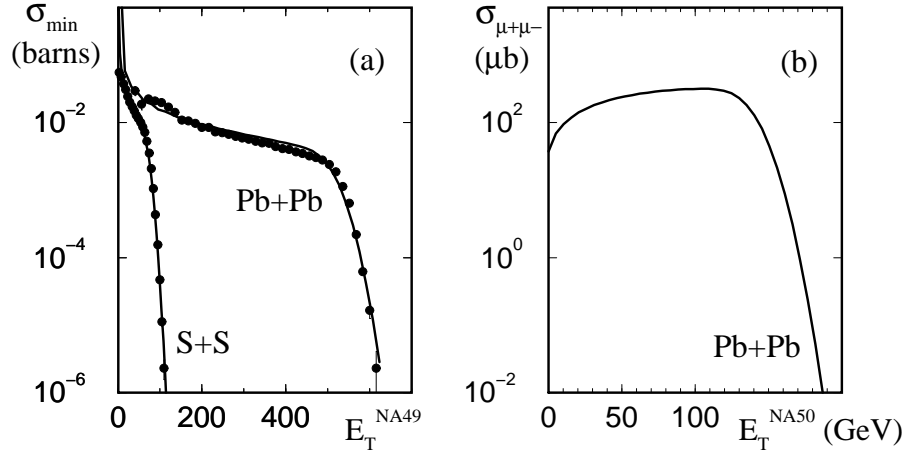

Figure 3. Transverse energy distributions from eqs. (7, 8). The S–Pb comparison (a) employs the same parameters.

and (6) to simulate the NA50 dimuon trigger. We take $\epsilon = 0.35$ GeV, $\omega = 3.2$, and $\sigma^{NN}_{\mu^+\mu^-} \approx 35.2$ pb as appropriate for the dimuon–mass range $2.9 < M < 4.5$ GeV. The E_T distribution for S+U $\to \mu^+\mu^- + X$ from NA38 was described [5] using $\epsilon = 0.64$ GeV and $\omega = 3.2$ – the change in ϵ corresponds roughly to the shift in particle production when the pseudorapidity coverage is changed from $1.7 < \eta < 4.1$ (NA38) to $1.1 < \eta < 2.3$ (NA50). Taking $\epsilon = 0.35$ GeV is the second update listed earlier. Though not shown here, we comment that the calculations agree with the NA50 data at high E_T, but differ somewhat at low E_T due to the efficiency of the active target, which is lower for more peripheral collisions.

We now apply eqs. (1,2,4) and (5) to charmonium suppression in Pb+Pb collisions. To determine nucleon absorption, we used pA data to fix $\sigma_{\psi N} \approx 4.8$ mb in Ref. [5]. This choice is in accord with the latest NA38 and NA51 pA data, see fig. 4a. To specify comover
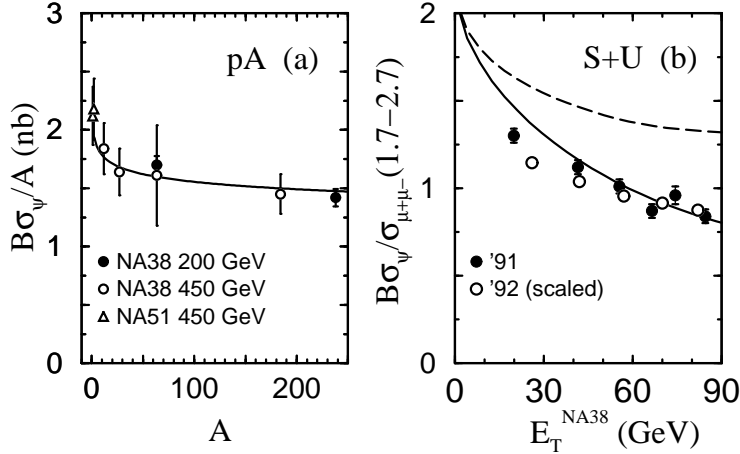

Figure 4. (a) pA cross sections [1] in the NA50 acceptance and (b) NA38 S+U ratios from the '91 [6] and '92 [1] runs. '92 data are scaled to the '91 continuum. The dashed line indicates the suppression from nucleon absorption alone.

scattering [5], we assumed that the dominant contribution to ψ dissociation comes from exothermic hadronic reactions such as $\rho + \psi \to D + \overline{D}$. We further took the comovers to evolve from a formation time $\tau_0 \sim 2$ fm to a freezeout time $\tau_F \sim R_T/v_{\rm rel}$ following Bjorken scaling, where $v_{\rm rel} \sim 0.6$ is roughly the average $\psi - \rho$ relative velocity. The survival probability, eq. (2), is then

$$S_{\rm co} = \exp\{-\sigma_{\rm co}v_{\rm rel}n_0\tau_0 \ln(R_T/v_{\rm rel}\tau_0)\} \tag{8}$$

where $\sigma_{\rm co} \approx 2\sigma_{\psi N}/3$, $R_T \approx R_A$ and n_0 is the initial density of sufficiently massive ρ, ω and η mesons. To account for the variation of density with E_T, we take $n_0 = \overline{n}_0 E_T/\overline{E}_T(0)$ [4]. A value $\overline{n}_0 = 0.8$ fm^{-3} was chosen to fit the central S+U datum. Since we fix the density in central collisions, this simple *ansatz* for $S_{\rm co}$ may be inaccurate for peripheral collisions.

We expect the comover contribution to the suppression to increase in Pb+Pb relative to S+U for central collisions because both the initial density and lifetime of the system can increase. To be conservative, we assumed that Pb and S beams achieve the same mean initial density. Even so, the lifetime of the system essentially doubles in Pb+Pb because $R_T \sim R_A$ increases to 6.6 fm from 3.6 fm in S+U. The increase in the comover contribution evident in comparing figs. 2 and 4b is described by the seemingly innocuous logarithm in eq. (8), which increases by $\approx 60\%$ in the larger Pb system.

In Ref. [5], we pointed out that comovers were necessary to explain S+U data from the NA38 1991 run [6]. Data just released [1] from their 1992 run support this conclusion. The '91 ψ data were presented as a ratio to the dimuon continuum in the low mass range $1.7 < M < 2.7$ GeV, where charm decays are an important source of dileptons. On the other hand, the '92 ψ data [1,9] are ratios to the Drell–Yan cross section in the range $1.5 < M < 5.0$ GeV. That cross section is extracted from the continuum by fixing the K–factor in the high mass region [14]. To compare our result from Ref. [5] to these data, we scale the '92 data by an empirical factor. This factor is $\approx 10\%$ larger than our calculated factor $\sigma_{DY}^{NN}(92)/\sigma_{\text{cont.}}^{NN}(91) \approx 0.4$; these values agree within the NA38 systematic errors. [NA50 similarly scaled the '92 data to the high–mass continuum to produce fig. 1.] Because our fit is driven by the highest E_T datum, we see from fig. 4b that a fit to the '92 data would not appreciably change our result. Note that a uniform decrease of the ratio by 10% would increase the comover contribution needed to explain S+U collisions.

NA50 and NA38 have also measured the total ψ–production cross section in Pb+Pb [1] and S+U reactions [7]. To compare to that data, we integrate eqs. (4, 6) to obtain the total $(\sigma/AB)_\psi = 0.97$ nb in S+U at 200 GeV and 0.54 nb for Pb+Pb at 158 GeV in the NA50 spectrometer acceptance, $0.4 > x_F > 0$ and $-0.5 < \cos\theta < 0.5$ (to correct to the full angular range and $1 > x_F > 0$, multiply these cross sections by ≈ 2.07). The experimental results in this range are $1.03 \pm 0.04 \pm 0.10$ nb for S+U collisions [6] and $0.44 \pm 0.005 \pm 0.032$ nb for Pb+Pb reactions [1]. Interestingly, in the Pb system we find a Drell–Yan cross section $(\sigma/AB)_{DY} = 35.2$ pb while NA50 finds $(\sigma/AB)_{DY} = 32.8 \pm 0.9 \pm 2.3$ pb. Both the ψ and Drell–Yan cross sections in Pb+Pb collisions are somewhat above the data, suggesting that the calculated rates at the NN level may be $\sim 20 - 30\%$ too large at 158 GeV. Such an error is consistent with ambiguities in current pp data near that low energy [11]. Note also that nuclear effects on the parton densities omitted in eqs. (4,5) can affect the total S and Pb cross sections at this level.

4. COMPARISON TO OTHER WORK

To compare more easily our results with those in Refs. [1,2], we present the following technical points. Blaizot and Ollitrault [2] and Kharzeev in these proceedings have observed that one can describe the measured total cross sections in pA and S+U in the absence of comovers if one takes $\sigma_{\psi N} = 6.2$ mb. We also find this to be true – neglecting comovers and taking their value for the absorption cross section, we obtain $(\sigma/AB)_\psi = 1.05$ nb in S+U at 200 GeV and 0.62 nb for Pb+Pb at 158 GeV. On the other hand, our calculated E_T–dependent ratios do *not* agree with measurements, as shown in fig. 5 (see also [5]). The importance of comovers in high E_T events follows from the correlation between E_T, centrality and particle (comover) multiplicity. On the other hand,
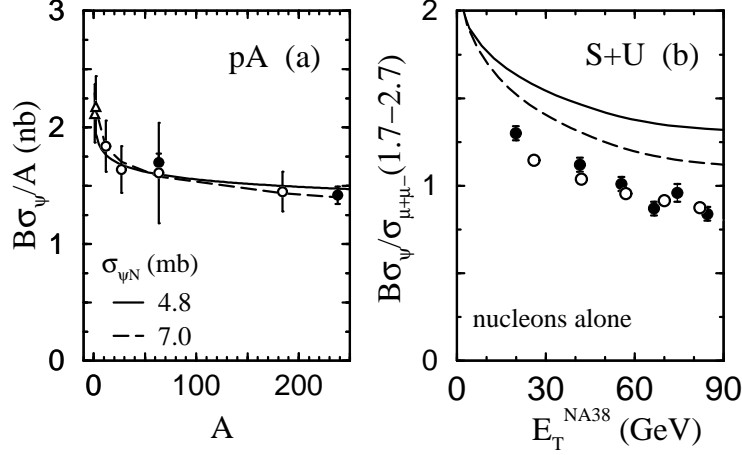
Figure 5. Suppression due to nucleon absorption alone using a value $\sigma_{\psi N} = 7$ mb as suggested by Kharzeev and Satz [2] does not describe S+U data (b). Both this value and our preferred 4.8 mb are consistent with pA data (a).

comovers only contribute to the total S+U cross section at the $\sim 18\%$ level, because the impact–parameter integrated cross section is dominated by large b and the distinction between central and peripheral interactions is more striking for the asymmetric S+U system.

How well does our value $\sigma_{\psi N} = 4.8$ mb agree with the pA data? We estimate the χ^2 per degree of freedom to be 0.34 for $\sigma_{\psi N} = 0.62$ mb and 1.3 for $\sigma_{\psi N} = 0.48$ mb. Both values of χ^2/d.o.f. are close to unity and indicate reasonable fits. Given the paucity of the data and the crudeness of the models, we consider the agreement to data to be equivalent. Observe that including the measured S+U total cross section in extracting $\sigma_{\psi N}$ from data as in [1] introduces an inappropriate bias.

Where does the $L(E_T)$ in NA50's plot come from and how does it approach the geometric? To address these questions we estimate $L(E_T)$. Following [10] we neglect comovers and equate (3) to our result for the ψ–to– continuum ratio from (1) and (4-6). We then expand in powers of $\sigma_{\psi N}$ and equate the terms proportional to $\sigma_{\psi N}$ to find

$$\rho_0 L(E_T) = \{2\overline{T}_{AB}\}^{-1} \int d^2b\, P(E_T, b) \int d^2s\, \{[T_A(s)]^2 T_B(b-s) + T_A(s)[T_B(b-s)]^2\} \qquad (9)$$

where

$$\overline{T}_{AB} \equiv \int d^2b\, P(E_T, b) \int d^2s\, T_A(s) T_B(b-s) \qquad (10)$$

and $T_A \equiv \int \rho_A dz$. This quantity is strictly meaningful for values of the mean free path $\rho_0 \sigma_{\psi N} \ll L$, as are the results of [10]. Following [1,10], we overlook the fact that this is not true for realistic parameter values, and obtain the result in fig. 6. We see that both our L and the average value of $\langle |b| \rangle$ obtained from $P(E_T, b)$ are in excellent accord with NA50 results in [1]. To compare to NA50, we calculate L for $\rho_0 \to 0.132$ fm^{-3} (a more
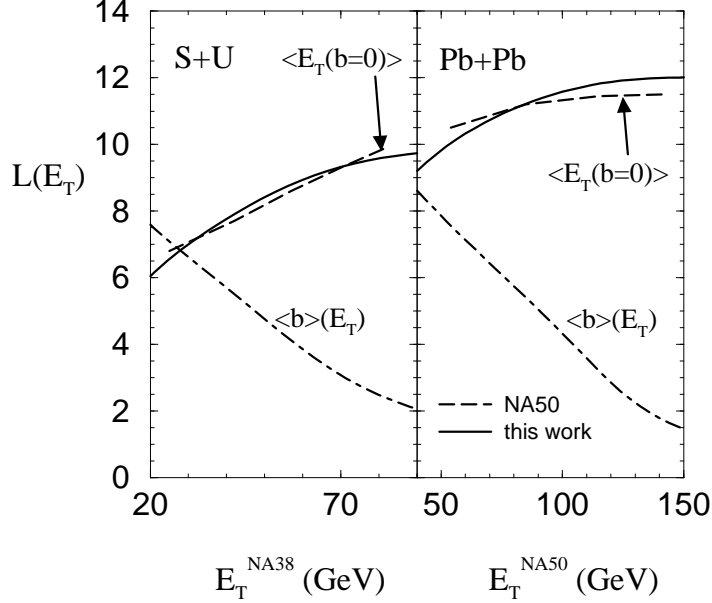
Figure 6. $L(E_T)$ for S+U and Pb+Pb from (9,10) (solid curve) is in good agreement with the NA50 result (dashed curve) used to create fig. 1 (dashed curve). The dot–dashed curve shows the average impact parameter b obtained from $P(E_T, b)$. The dashed line begins and ends at centroids of the lowest and highest E_T bins measured.

realistic value is 0.17 fm^{-3}). More importantly, we see that saturation is nearly achieved in the symmetric Pb+Pb system even when the average b is rather large.

5. ψ' SUPPRESSION

To apply eqs. (4-6) to calculate the ψ'–to–ψ ratio as a function of E_T, we must specify $\sigma_{\psi'}^{NN}$, $\sigma_{\psi'N}$, and $\sigma_{\psi'\text{co}}$. Following Ref. [11], we use pp data to fix $B\sigma_{\psi'}^{NN}/B\sigma_{\psi}^{NN} = 0.02$ (this determines $F_{\psi'}$). The value of $\sigma_{\psi'N}$ depends on whether the nascent ψ' is a color singlet hadron or color octet $c\bar{c}$ as it traverses the nucleus. In the singlet case, one expects the absorption cross sections to scale with the square of the charmonium radius. Taking this ansatz and assuming that the ψ' forms directly while radiative χ decays account for 40% of ψ production, one expects $\sigma_{\psi'} \sim 2.1\sigma_{\psi}$ for interactions with either nucleons or comovers [5]. For the octet case, we take $\sigma_{\psi'N} \approx \sigma_{\psi N}$ and fix $\sigma_{\psi'\text{co}} \approx 12$ mb to fit the S+U data. In fig. 5a, we show that the singlet and octet extrapolations describe pA data equally well.

Our predictions for Pb+Pb collisions are shown in fig. 6. In the octet model, the entire suppression of the ψ'–to–ψ ratio is due to comover interactions. In view of the schematic nature of our approximation to S_{co} in eq. (8), we regard the agreement with data of singlet and octet extrapolations as equivalent.
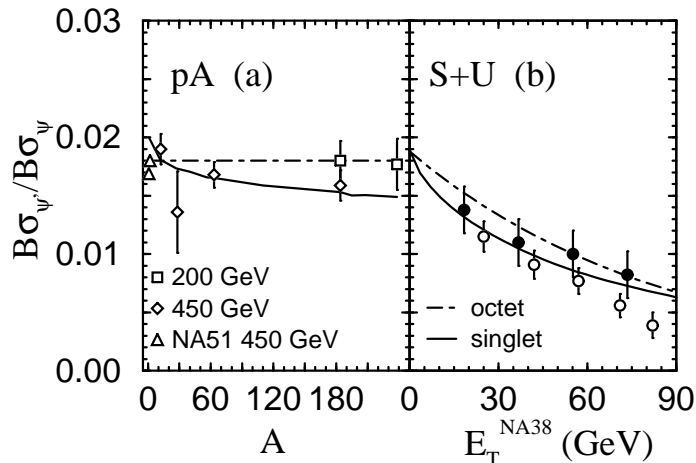
Figure 7. Comover suppression of ψ' compared to (a) NA38 and NA51 pA data [1, 9] and (b) NA38 S+U data [8] (filled points) and preliminary data [1].

6. SUMMARY

In summary, the Pb data [1] cannot be described by nucleon absorption alone. This is seen in the NA50 plot, fig. 1, and confirmed by our results. The saturation with L but not E_T suggests an additional density–dependent suppression mechanism. Earlier studies pointed out that additional suppression was already needed to describe the S+U results [5]; recent data [1] support that conclusion (see, however, [2]). To study the S+U question further, experiments can search for saturation in super–central S+U reactions. More generally, while comover scattering explains the additional suppression, it is unlikely that that explanation is unique. SPS inverse–kinematics experiments ($B < A$) and AGS pA studies near the ψ threshold [15] can help pin down model uncertainties.

In the context of our hadronic scenario, the success of the ψ and ψ' predictions imply comover densities perhaps exceeding ~ 1 fm^{-3} in Pb+Pb collisions. Similar densities are found in string and cascade models of heavy ion collisions. We must ask if such hadronic models are applicable at such densities — they must certainly be at the very edge of their applicability. Nevertheless, such models have proven very useful as predictive phenomenological tools. The ability to predict hadronic backgrounds that we have demonstrated is a prerequisite for using charmonium to search for new phenomena at RHIC and LHC.

REFERENCES
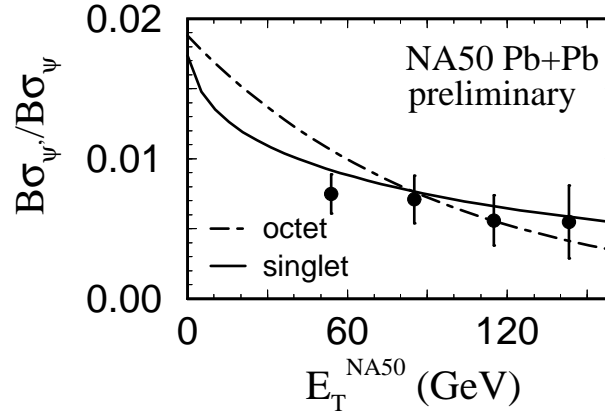
Figure 8. Comover suppression in Pb+Pb $\to \psi' + X$.

1. M. Gonin *et al.* (NA50), Proc. Quark Matter '96, Heidelberg, Germany, P. Braun-Munzinger *et al.*, eds. (1996).
2. J.-P. Blaizot and J.-Y. Ollitrault, (1996) hep-ph/9606289; D. Kharzeev and H. Satz, Proc. Quark Matter '96, *op cit.*; A. Capella, private communication.
3. S. Gavin and R. Vogt, LBL-37980 (1996), hep-ph/9606560.
4. S. Gavin and R. Vogt, Nucl. Phys. B345 (1990) 104.
5. S. Gavin, H. Satz, R. L. Thews, and R. Vogt, Z. Phys. C61 (1994) 351; S. Gavin, Nucl. Phys. A566 (1994) 287c.
6. O. Drapier *et al.* (NA38) Nucl. Phys. A544 (1992) 209c.
7. C. Baglin *et al.* (NA38) Phys. Lett. B270 (1991) 105.
8. C. Baglin *et al.* (NA38) Phys. Lett. B345 (1995) 617; S. Ramos *et al.* Nucl. Phys. A590 (1995) 117c.
9. C. Lourenco (NA38/NA50), Europhysics Conf. on High Energy Physics - EPS-HEP, Brussels (1995).
10. C. Gerschel and J. Hüfner, Z. Phys. C56 (1992) 171.
11. R. Gavai *et al.*, Int. J. Mod. Phys. A10 (1995) 3043.
12. S. Gavin *et al.*, Int. J. Mod. Phys. A10 (1995) 2961.
13. S. Margetis *et al.* (NA49), Phys. Rev. Lett. 75 (1995) 3814.
14. M.C. Abreu *et al.*, Nucl. Phys. A566 (1994) 77c.
15. K. Seth, Proc. Int. Conf. on Flavor and Spin in Hadronic Physics, Torino, eds. F. Balestra *et al.* (Editrice Compositori, Bologna, 1994).